Metallacarboranes derived from the $[C_2B_{10}H_{12}]^{2-}$ Anion. The Preparation, Molecular Structure, and Properties of [4-(dppe)-4-Pd-1,6-$C_2B_{10}H_{12}$], [4,4,4-H(PPh_3)$_2$-2-OMe-4-Ir-1,6-$C_2B_{10}H_{11}$], and [3-(dppe)-3-Pt-1,2-$C_2B_9H_{11}$]†

Nathaniel W. Alcock, John G. Taylor, and Malcolm G. H. Wallbridge*
Department of Chemistry, University of Warwick, Coventry CV4 7AL

The action of $Na_2[C_2B_{10}H_{12}]$ on $[PdCl_2(dppe)]$ (dppe = $Ph_2PCH_2CH_2PPh_2$) yields the 13-vertex yellow *closo* species $[(dppe)PdC_2B_{10}H_{12}]$ (**1**), and the reaction of $[NMe_4][C_2B_{10}H_{13}]$ with $[IrCl(PPh_3)_3]$ in light petroleum–methanol gives a related 13-vertex cage of yellow $[(PPh_3)_2HIrC_2B_{10}H_{11}(OMe)]$ (**2**), whose formation involves attack by a solvent molecule. The structure of both products have been established by *X*-ray diffraction [*R* = 0.039 and 0.074 for 4 786 and 4 130 diffractometer-measured observed reflections, for (**1**) and (**2**) respectively]. Both show the characteristic 1 : 5 : 6 : 1 structure for 13-vertex polyhedra, distorted by carbon substitution. The reaction of $Tl(O_2CMe)$ with $Na_2[C_2B_{10}H_{12}]$ in ethanol leads to degradation of the C_2B_{10} cage, and yields an orange solid formulated as $Tl_3(C_2B_9H_{12})O$. Treatment of this solid with $[PtCl_2(dppe)]$ gives the pale orange $[(dppe)PtC_2B_9H_{11}]$ (**3**); it has an icosahedral structure [*R* = 0.068 for 3 530 observed reflections], distorted mainly by the lengthening of the Pt–C bonds in comparison to the Pt–B bonds.

The study of metalla-borane and -carborane derivatives continues to be an active area of research, and has recently been reviewed.[1] We are interested in the effects resulting from the insertion of electron-rich metals (*e.g.* those of Group 8 and subsequent groups) into carborane frameworks, since such species often show considerable distortions in the resulting metallacarborane.[2] While such distortions are now well known for the 12-vertex MC_2B_9 systems, we were interested to see whether similar distortions would occur in 13-vertex MC_2B_{10} cages. Such derivatives can be easily obtained by the reaction of a metal halide derivative with the borane or carborane anion, often as the alkali-metal salt. For example, the anion $[C_2B_{10}H_{12}]^{2-}$ can be obtained conveniently by the action of sodium in tetrahydrofuran (thf) on the icosahedral carborane 1,2-$C_2B_{10}H_{12}$.[3] Although the structure of this anion is as yet unknown, several metalla-derivatives have been characterised,[1,4,5] although detailed structural data are only available for the titanium(IV)[6] and cobalt(III)[7] derivatives (Scheme).

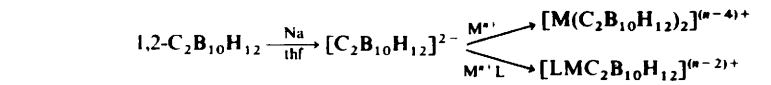

Scheme. M = Ti, Zr, Hf, V, Cr, Mo, W, Mn, Fe, Co, or Ni; L = η-C_5H_5 or $(CO)_3$

We now report the preparation, properties, and structures of derivatives containing the electron-rich Group 8 metals palladium and iridium, and also the results of attempts to prepare the thallium salt of $[C_2B_{10}H_{12}]^{2-}$. This salt is expected to be a useful precursor in the preparation of other metalla-derivatives, as is found for the corresponding salt $Tl_2[C_2B_9H_{11}]$.[8]

† 4-[1′,2′-Bis(diphenylphosphino)ethane]-*closo*-1,6-dicarba-4-palladatridecaborane, 4-hydrido-2-methoxo-4,4-bis(triphenylphosphine)-*closo*-1,6-dicarba-4-iridatridecaborane, and 3-[1′,2′-bis(diphenylphosphino)ethane]-*closo*-1,2-dicarba-3-platinadodecaborane, respectively. (The numbering system employed is as suggested in J. B. Casey, W. J. Evans, and W. H. Powell, *Inorg. Chem.*, 1981, **20**, 1333.)

Supplementary data available: see Instructions for Authors, *J. Chem. Soc., Dalton Trans.*, 1987, Issue 1, pp. xvii—xx.

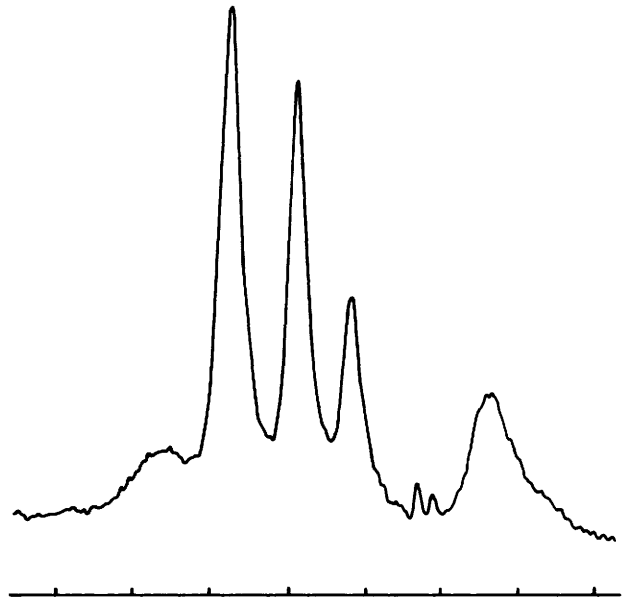

Figure 1. The 128-MHz ^{11}B-$\{^1H\}$ n.m.r. spectrum of [(dppe)Pd-$C_2B_{10}H_{12}$] in dichloromethane

Results and Discussion

The addition of $[PdCl_2(dppe)]$ [dppe = 1,2-bis(diphenylphosphino)ethane] to a dichloromethane solution of $Na_2[C_2B_{10}H_{12}]$ gives an initial red colour. On filtration in air the solution slowly changes to a straw yellow colour, and yellow crystals of $[(dppe)PdC_2B_{10}H_{12}]$ (**1**) were obtained after purification. Colour changes have been observed previously in transition-metal derivatives of the $[C_2B_{10}H_{12}]^{2-}$ ion, and have been ascribed to the facile interconversion of structural isomers.[4] Since it appears unlikely that this colour change is associated with oxidation of the metal ion, we assume that structural changes probably occur in this case also.

The difficulty of assigning a plausible structure to the

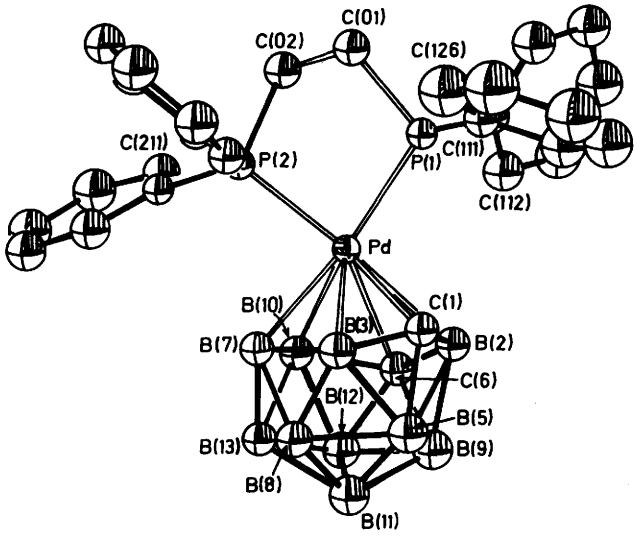

Figure 2. Molecular structure of $[(dppe)PdC_2B_{10}H_{12}]$, (1) showing the crystallographic atomic numbering. Hydrogen atoms are omitted for clarity here and elsewhere

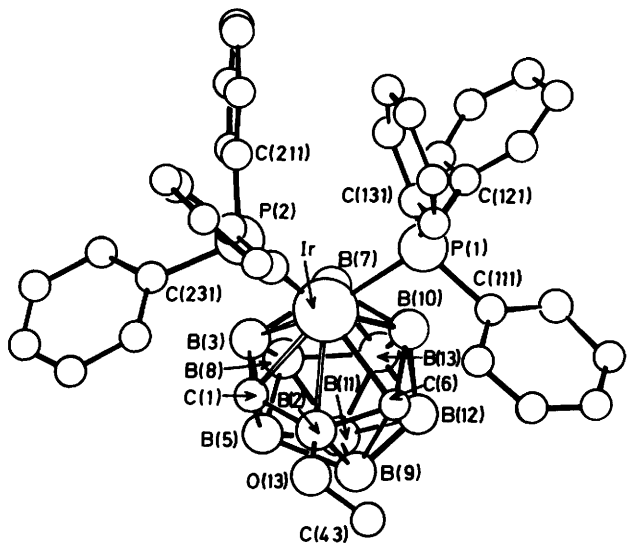

Figure 3. Molecular structure of $[(PPh_3)_2HIrC_2B_{10}H_{11}(OMe)]$ (2) showing the crystallographic atomic numbering

MC_2B_{10} framework from n.m.r. data alone has been reported previously,[4,7] and (1) presents similar difficulties. The best resolved ^{11}B-$\{^1H\}$ n.m.r. spectrum at 128 MHz showed a series of five broad overlapping resonances (Figure 1), and the integration based on a fragment containing ten boron atoms is unclear. While the ratio of the four resonances between +5 and −10 p.p.m. to that near −18 p.p.m. is approximately 8:2 (actually 8.8:2), the individual ratios of the lower-field set of four resonances are approximately 1:3:2:1. Since this group of resonances apparently represents eight boron atoms we assume that the overlap of the resonances causes this anomaly. The resonances broaden considerably at lower temperatures, thus at −90 °C in CH_2Cl_2 the resonance at −1 p.p.m. is over 800 Hz wide at half-height. Fluxionality in such 13-vertex systems has been observed previously,[4] and has been reasonably suggested to arise from an interchange between isomeric species which have the carbon atoms of the C_2B_4 face in alternative positions, it being assumed that the interchange proceeds *via* the square–diamond–square process. Since we were unable to make any structural assignment from the n.m.r. data a crystal-structure determination was undertaken.

The resulting structure (Figure 2) confirms the presence of a 13-vertex metallacarborane *closo* cluster, and shows that the two carbon atoms are separated by a boron atom in the six-membered C_2B_4 face; this feature is similar to that observed previously in $[NMe_4]_2[Ti(C_2B_{10}H_{10}Me_2)_2]$[6] and $[(\eta\text{-}C_5H_5)Co(C_2B_{10}H_{12})]$.[7] While there is no strong distortion of the fragment containing the d^8 Pd^{II} and the C_2B_4 face, some asymmetry is evident (see below).

A related yellow iridium derivative, $[(PPh_3)_2HIrC_2B_{10}H_{11}(OMe)]$ (2) was prepared by refluxing $[IrCl(PPh_3)_3]$ and $[NMe_4][C_2B_{10}H_{13}]$ in light petroleum (b.p. 60—80 °C)–methanol. Refluxing the two reagents for 1 h in light petroleum alone produced no colour change. The ^{11}B n.m.r. spectrum (CH_2Cl_2 solution) showed a series of broad overlapping resonances (at least three in number) between +17 and +2 p.p.m., and as with (1) was unhelpful for structural assignment. A crystal-structure determination (Figure 3) revealed that an unexpected solvolysis had taken place replacing one cage B–H hydrogen by –OMe, and that (2) is the 13-vertex *closo* species $[(PPh_3)_2HIrC_2B_{10}H_{11}(OMe)]$. As with (1) the two carbon atoms are separated by a boron atom; further structural details are discussed below. The presence of the methoxy group is perhaps not too surprising since other examples are known where methoxy groups are substituted into metallaboranes when the compounds are formed in alcoholic solution.[9] Predictably the methoxy group substitutes at the boron atom which adjoins the two carbon atoms and the metal atom.

We have also attempted to prepare the thallium derivative $Tl_2[C_2B_{10}H_{12}]$ by reacting $Na_2[C_2B_{10}H_{12}]$ with thallium(I) acetate, since it is known that a similar reaction using $Na_2[C_2B_9H_{11}]$ yields $Tl_2[C_2B_9H_{11}]$.[8] In the present work the interaction of an ethanol solution of thallium(I) acetate with $Na_2[C_2B_{10}H_{12}]$ in thf produced a flocculent orange precipitate. The material appeared to be heat sensitive, since attempts to coagulate the suspension by heating caused some darkening. Although the heating was carried out in the light, we have observed that the precipitate is not light sensitive, at least over a few hours. However, the precipitate could be filtered off, and after drying under vacuum yielded an orange solid. No satisfactory n.m.r. spectra could be obtained from the solid due to insolubility, but elemental analysis was not consistent with the formulation $Tl_2[C_2B_{10}H_{12}]$. In view of the analytical data, and the reactions described below, it appears that a cage degradation has occurred, and the best formulation we can propose for the solid is $Tl_3(C_2B_9H_{12})O$.

When the orange solid is suspended in thf, and treated with $[PMePh_3]Br$, the mixture slowly darkens and a black solid is precipitated. A pale yellow solid can be recovered in high yield from the supernatant after filtration, and this solid corresponds to $[PMePh_3][C_2B_9H_{12}]$ from analytical data and the ^{11}B n.m.r. spectrum. The latter shows doublets at −9.44 (relative intensity 2), −15.2 (2), −16.2 (1), −20.8 (2), −31.6 (1), and −36.4 (1) p.p.m.; these values are very similar to those for $[C_2B_9H_{12}]^-$ reported previously.[10] The i.r. spectrum of the solid shows the expected absorptions from the cation, but also gives a broad band at 2 500 cm^{-1} whose contour is similar to that reported for the $[C_2B_9H_{12}]^-$ ion.[10] We assume that the black solid produced is Tl_2O, and that the overall reaction proceeds as follows.

$$Tl_3(C_2B_9H_{12})O + [PMePh_3]Br \longrightarrow [PMePh_3][C_2B_9H_{12}] + Tl_2O + TlBr$$

The base degradation of $C_2B_{10}H_{12}$ to $[C_2B_9H_{12}]^-$ occurs readily when the former is treated with an NaOEt–EtOH

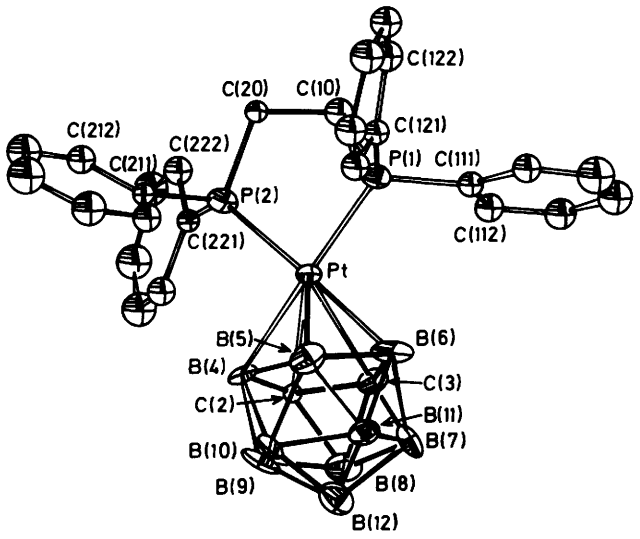

Figure 4. Molecular structure of $[(dppe)PtC_2B_9H_{11}]$ (**3**) showing the crystallographic atomic numbering

mixture.[10] In the present work the acetate ion appears to have the same effect as alkoxide, and indeed we have confirmed that even an $Li(O_2CMe)$–EtOH mixture carries out this degradation. The alternative pathways involving the formation and decomposition of an intermediate 13-vertex metallacarborane appear less likely, though such a route has been proposed to explain the formation of $[(\eta\text{-}C_5H_5)Co(C_2B_9H_{11})]$ from the direct action of $[Co(CO)_2(\eta\text{-}C_5H_5)]$ on $C_2B_{10}H_{12}$.[11]

The presence of a C_2B_9 fragment in the orange thallium derivative is also indicated by its interaction with $[PtCl_2(dppe)]$. The yellow-orange complex $[(dppe)PtC_2B_9H_{11}]$ (**3**) was isolated from the reaction mixture, and tentatively identified from its ^{11}B n.m.r. spectrum by comparison with those previously reported for similar PtC_2B_9 cage compounds which have the two carbon atoms occupying adjacent positions in the cage.[2,12] However, since the spectrum shows broad overlapping resonances [+10.1 (relative intensity 1), −10.3 (5), and −21.5 (3)], an *X*-ray structure determination was undertaken to confirm this identification (Figure 4).

Structural Results.—While the 13-vertex MC_2B_{10} polyhedra in (**1**) and (**2**) are necessarily rather irregular, they share the same overall geometry, which is also common to the two previous 13-vertex structures reported.[6,7] This can best be seen from a diagram of connectivity and distances (Figure 5; *cf.* Figure 3 in ref. 7), which shows the overall pseudo-mirror symmetry of the polyhedra.[6] However, there are interesting differences between both (**1**) and (**2**), and the well defined cobalt compound. Despite the different metal electron configurations in (**1**) (d^8) and (**2**) (d^6) there are some similarities in the pattern of M–cage bonds (Figure 6 and Table 1). Each has the shortest link to the unique low-co-ordinate carbon atom [C(1)], and both have a significantly longer bond to an atom one away from this unique carbon. In (**1**) this link is to the other carbon [Pd–C(6)], while in (**2**) it is to a boron atom [Ir–B(7)]; the remaining facial bonds are relatively short. This indicates both that the top C_2B_4 layers of the cages are similar in their distortions, and that the metal atoms are attached in very much the same position relative to the centroid of the open face. In contrast, in the cobalt compound, although the Co–C(unique) bond is still the shortest, all the other M–facial bond lengths are comparable. The compounds (**1**) and (**2**) do show a significant difference because of the presence of the hydride ligand on Ir. In (**1**), the P(1)–Pd–P(2) plane is almost perpendicular to the mean

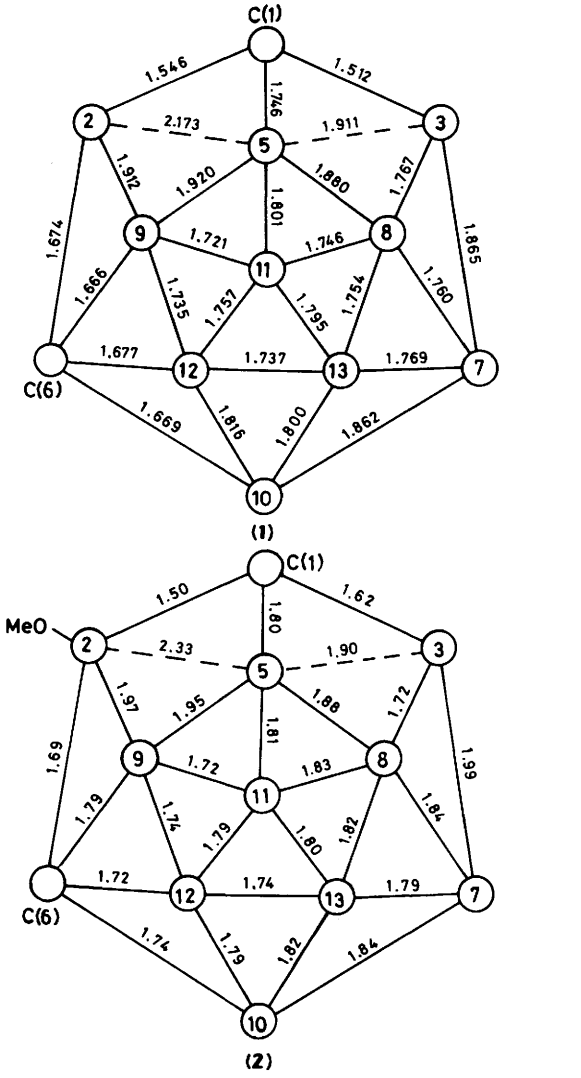

Figure 5. Schematic representations of the carborane fragments in compounds (**1**) and (**2**). The atom numbers relate to boron unless otherwise indicated, bond distances in Å

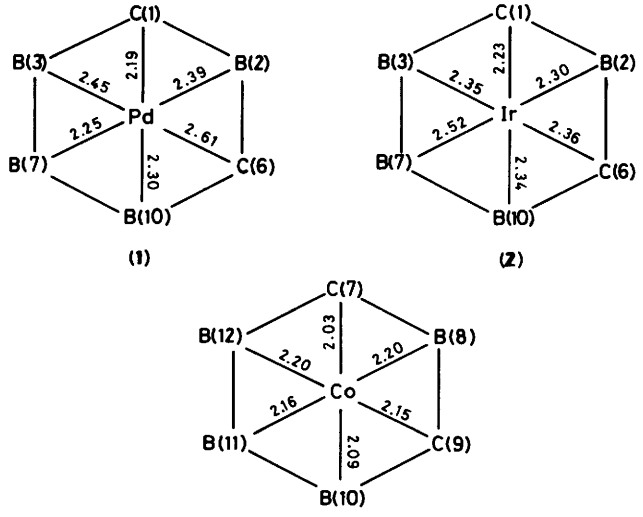

Figure 6. Schematic representation of of the M–cage bonding in compounds (**1**), (**2**), and $[(\eta\text{-}C_5H_5)Co(C_2B_{10}H_{12})]$, bond distances in Å

Table 1. Principal bond lengths (Å) and angles (°) for compounds (**1**), (**2**), and (**3**)

Compound (**1**)

Pd–P(1)	2.317(1)	B(2)–C(6)	1.674(6)	B(7)–B(13)	1.769(7)	B(13)–B(11)	1.795(8)
Pd–P(2)	2.252(1)	B(2)–B(9)	1.912(7)	B(7)–B(8)	1.760(7)	B(12)–B(9)	1.735(8)
Pd–B(2)	2.387(5)	B(2)–B(5)	2.173(7)	B(10)–C(6)	1.669(7)	B(12)–B(11)	1.757(7)
Pd–C(1)	2.187(5)	C(1)–B(3)	1.512(8)	B(10)–B(13)	1.800(8)	B(9)–B(5)	1.920(7)
Pd–B(3)	2.455(5)	C(1)–B(5)	1.746(8)	B(10)–B(12)	1.816(7)	B(9)–B(11)	1.721(9)
Pd–B(7)	2.252(6)	B(3)–B(7)	1.865(7)	C(6)–B(12)	1.677(7)	B(5)–B(8)	1.880(9)
Pd–B(10)	2.300(4)	B(3)–B(5)	1.911(7)	C(6)–B(9)	1.666(7)	B(5)–B(11)	1.801(7)
Pd–C(6)	2.609(4)	B(3)–B(8)	1.767(7)	B(13)–B(12)	1.737(8)	B(8)–B(11)	1.746(7)
B(2)–C(1)	1.546(7)	B(7)–B(10)	1.862(6)	B(13)–B(8)	1.754(6)		

Compound (**2**)

Ir–P(1)	2.340(5)	B(2)–B(9)	1.97(3)	C(1)–B(3)	1.62(3)	B(13)–B(8)	1.82(3)
Ir–P(2)	2.312(4)	B(2)–B(5)	2.33(3)	B(7)–B(10)	1.84(3)	B(13)–B(11)	1.80(3)
Ir–B(2)	2.305(18)	B(2)–O(13)	1.43(2)	B(7)–B(13)	1.79(3)	B(12)–B(9)	1.74(3)
Ir–C(1)	2.230(16)	O(13)–C(43)	1.44(3)	B(7)–B(8)	1.84(3)	B(12)–B(11)	1.79(3)
Ir–B(3)	2.350(25)	C(1)–B(3)	1.62(3)	B(10)–C(6)	1.74(3)	B(9)–B(5)	1.95(3)
Ir–B(7)	2.520(15)	C(1)–B(5)	1.80(3)	B(10)–B(13)	1.82(3)	B(9)–B(11)	1.72(4)
Ir–B(10)	2.336(22)	B(3)–B(7)	1.99(3)	B(10)–B(12)	1.79(3)	B(5)–B(8)	1.88(4)
Ir–C(6)	2.360(15)	B(3)–B(5)	1.90(3)	C(6)–B(12)	1.72(3)	B(5)–B(11)	1.81(3)
B(2)–C(6)	1.69(3)	B(3)–B(8)	1.72(3)	C(6)–B(9)	1.79(3)	B(8)–B(11)	1.83(3)
B(2)–C(1)	1.50(3)			B(13)–B(12)	1.74(3)		

Compound (**3**)

Pt–P(1)	2.266(3)	C(2)–B(4)	1.74(3)	B(4)–B(10)	1.83(3)	B(7)–B(12)	1.81(3)
Pt–P(2)	2.259(3)	C(2)–B(8)	1.71(3)	B(5)–B(6)	1.83(3)	B(8)–B(9)	1.74(3)
Pt–C(2)	2.502(3)	C(2)–B(9)	1.63(3)	B(5)–B(10)	1.81(3)	B(8)–B(12)	1.77(3)
Pt–C(3)	2.505(3)	C(3)–B(6)	1.79(3)	B(5)–B(11)	1.75(3)	B(9)–B(10)	1.78(3)
Pt–B(4)	2.251(3)	C(3)–B(7)	1.67(3)	B(6)–B(7)	1.85(3)	B(9)–B(12)	1.80(3)
Pt–B(5)	2.279(3)	C(3)–B(8)	1.76(3)	B(6)–B(11)	1.85(3)	B(10)–B(11)	1.77(3)
Pt–B(6)	2.255(3)	B(4)–B(5)	1.83(3)	B(7)–B(8)	1.79(3)	B(10)–B(12)	1.79(3)
C(2)–C(3)	1.53(3)	B(4)–B(9)	1.81(3)	B(7)–B(11)	1.79(3)	B(11)–B(12)	1.79(3)

P–M–P	(1) 84.9(1)	(2) 97.2(2)	(3) 84.7(1)

B–M–P angles	(1)	(2)	(3)		(1)	(2)	(3)
Smallest to P(1)	97.4(1)	79.5(6)	97.1(2)	Largest to P(1)	165.1(1)	164.3(5)	171.6(2)
from	B(2)	B(10)	B(6)	from	B(7)	C(1)	B(4)
Smallest to P(2)	89.8(1)	88.6(4)	99.9(2)	Largest to P(2)	166.8(1)	165.5(4)	178.3(2)
from	B(7)	B(3)	B(4)	from	B(2)	C(6)	B(6)

plane through the atoms of the open face (dihedral angle 92°), but in (**2**) the corresponding P(1)–Ir–P(2) plane is inclined substantially to one side (dihedral angle 74°), allowing space for a third ligand atom (the hydride) to be attached to the Ir.

Both (**1**) and (**2**) share the overall planarity of the B_3C section of the face B(3), B(7), B(10), C(6) with the unique carbon atom [C(1)] somewhat above this plane. It is clear therefore that although distortions are observed in the MC_2B_4 fragment of the cage, they are less marked than in the MC_2B_9 cages.

The attachment of the six-vertex upper plane to the five-vertex lower plane is achieved by opening out two adjacent faces so that each becomes a quadrilateral with long diagonals. The mirror symmetry is not exact, because of the asymmetrical placing of the two carbon atoms in a C–B–C arrangement around the six-vertex face, with one carbon on the pseudo-mirror plane. The presence of the second carbon causes bond shortening in the lower part of the cage, though only to a modest extent. The additional perturbation in (**2**) of the –OMe group attached to B(2) may shorten the bonds from B(2) slightly, but the precision of the structure determination is insufficient to be confident about this conclusion. In addition the presence of the methoxy group may be responsible for the substantial lengthening of bonds on the other side of the cage in (**2**) in comparison to (**1**). Viewed more generally, complexes (**1**) and (**2**) confirm that 13-membered metallacarboranes adopt a single specific cage geometry, even if individual compounds show slightly different distortions.

The structure of (**3**) is more straightforward than those of (**1**) and (**2**). The *nido*-C_2B_9 cage is completed by the Pt atom to give a *closo* icosahedron. The geometry of systems of this type has recently been examined in detail,[2] and shown to be affected by the *d* electron count of the metal, with the M–B bonds shortening and the M–C bonds lengthening as the number of *d* electrons increases. One other closely related d^8 platinum(II) complex has been examined, $[(PEt_3)_2PtC_2B_9H_{11}]$,[12] where the two carbon atoms in the cage are adjacent, and the dimensions of complex (**3**) are indistinguishable from this earlier example, indicating that the change in phosphine has no effect, even on the Pt–cage bonds.

Experimental

All reactions were performed under a nitrogen atmosphere using standard Schlenk-line techniques. Solvents were distilled immediately prior to use from either $LiAlH_4$ or sodium–benzophenone (thf). Infrared spectra were recorded using a Perkin-Elmer 580B spectrophotometer with Nujol mulls. The ^{11}B n.m.r. spectra were obtained at 128 MHz on a Bruker WH-400

Table 2. Crystallographic data

Compound	(1)	(2)	(3)
Formula	$C_{28}H_{36}B_{10}P_2Pd{\cdot}CH_2Cl_2$	$C_{39}H_{45}B_{10}IrOP_2{\cdot}CHCl_3$	$C_{28}H_{35}B_9P_2Pt$
M	773.9	1 011.4	725.9
System	Triclinic	Triclinic	Monoclinic
Space group	$P\bar{1}$	$P\bar{1}$	$P2_1/n$
Absences	None	None	$h0l$, $h + l \neq 2n$ $0k0$, $k \neq 2n$
a/Å	11.645(4)	9.922(2)	14.181(2)
b/Å	10.399(4)	11.068(2)	21.443(5)
c/Å	14.975(5)	20.433(3)	11.412(2)
α/°	100.71(3)	95.26(1)	90
β/°	104.24(3)	90.25(1)	99.83(1)
γ/°	94.45(3)	101.14(1)	90
U/Å^3	1 713(1)	2 191.8(7)	3 419(1)
D_c/g cm^{-3}	1.42	1.53	1.41
D_m/g cm^{-3}	1.38	1.52	1.53
Z	2	2	4
μ(Mo-K_α)/cm^{-1}	8.1	22.3	42.1
F(000)	748	1 004	1 448
Reflections:			
Total	6 056	5 100	6 548
$I/\sigma(I) \geqslant 3.0$	4 786	4 130	3 530
$2\theta_{max.}$/°	50	50	50
Range (2θ) about $\alpha_1 - \alpha_2$/°	±1.1	±1.1	±1.0
Min. speed (2θ)/° min^{-1}	2.0	1.2	2.0
T/K	290	290	173
Crystal size/mm	0.23 × 0.48 × 0.32	0.28 × 0.07 × 0.18	0.21 × 0.14 × 0.42
Transmission factors			
Max.—min.	0.55—0.39	0.89—0.76	0.79—0.61
g	0.007	0.007	Unit weights
R	0.039	0.074	0.068
R'	0.043	0.077	

Table 3. Final atomic co-ordinates (× 10^4) for compound (1)

Atom	x	y	z	Atom	x	y	z
Pd	1 313.1(2)	2 369.5(2)	2 175.3(2)	C(111)	2 733(4)	3 603(4)	586(3)
P(1)	2 335(1)	4 006(1)	1 701(1)	C(112)	2 486(4)	2 318(4)	43(3)
P(2)	−227(1)	3 557(1)	1 911(1)	C(113)	2 776(6)	2 036(5)	−794(3)
Cl(1)	3 522(3)	−1 814(3)	5 870(2)	C(114)	3 320(5)	3 021(6)	−1 116(3)
Cl(2)	3 991(4)	885(4)	6 892(3)	C(115)	3 547(4)	4 309(5)	−593(3)
C(012)	2 830(13)	−508(15)	6 033(10)	C(116)	3 258(4)	4 592(5)	255(3)
C(013)	2 738	286	6 594	C(121)	3 716(4)	4 827(4)	2 555(3)
C(015)	4 330	749	7 045	C(122)	4 779(4)	4 385(5)	2 485(4)
C(017)	3 547	758	6 184	C(123)	5 817(5)	4 906(6)	3 168(4)
C(018)	3 509	0	5 798	C(124)	5 805(5)	5 833(7)	3 915(4)
C(020)	3 530	0	5 813	C(125)	4 774(6)	6 301(8)	3 979(5)
C(01)	1 342(4)	5 278(4)	1 515(3)	C(126)	3 723(5)	5 811(6)	3 306(4)
C(02)	65(4)	4 599(4)	1 104(3)	C(211)	−1 754(4)	2 779(4)	1 419(3)
B(2)	2 700(5)	804(5)	2 111(4)	C(212)	−2 248(4)	2 417(4)	444(3)
C(1)	2 791(4)	1 667(5)	3 091(4)	C(213)	−3 409(4)	1 823(4)	76(3)
B(3)	1 926(4)	1 714(5)	3 698(3)	C(214)	−4 106(4)	1 572(4)	671(4)
B(7)	357(5)	1 202(5)	2 963(3)	C(215)	−3 620(4)	1 890(5)	1 640(4)
B(10)	170(4)	335(4)	1 721(3)	C(216)	−2 453(4)	2 503(4)	2 009(3)
C(6)	1 414(4)	−88(4)	1 446(3)	C(221)	−230(4)	4 781(4)	2 947(3)
B(13)	12(5)	−536(5)	2 625(4)	C(222)	683(4)	4 941(4)	3 781(3)
B(12)	642(5)	−1 282(4)	1 756(4)	C(223)	740(5)	5 968(5)	4 535(3)
B(9)	2 189(5)	−976(5)	2 141(4)	C(224)	−96(5)	6 843(4)	4 472(3)
B(5)	2 601(5)	129(5)	3 382(4)	C(225)	−994(5)	6 684(4)	3 659(4)
B(8)	1 117(5)	189(5)	3 665(3)	C(226)	−1 057(4)	5 659(4)	2 892(3)
B(11)	1 394(5)	−1 207(5)	2 939(4)				

spectrometer using $BF_3{\cdot}Et_2O$ as an external standard, with high-field resonances being quoted as negative values. The reagents $[MCl_2(dppe)]$ (M = Pd or Pt) and $[IrCl(PPh_3)_3]$ were prepared by literature methods.[13,14] Microanalyses were carried out by Butterworth Laboratories Ltd.

Preparation of $[(dppe)PdC_2B_{10}H_{12}]$ (**1**).—The carborane 1,2-$C_2B_{10}H_{12}$ (0.33 g, 2.3 mmol) was dissolved in thf (30 cm^3) containing small pieces of sodium (0.11 g, 4.6 mmol), and a catalytic trace of naphthalene. Stirring was continued until the sodium had reacted (*ca.* 2—3 h), and the clear solution was then evaporated. The residue was dissolved in degassed CH_2Cl_2 (30 cm^3), and then $[PdCl_2(dppe)]$ (1.33 g, 2.3 mmol) was added slowly to the stirred solution. The resulting dark red solution

Table 4. Final atomic co-ordinates (× 10^4) for compound (**2**)

Atom	*x*	*y*	*z*	Atom	*x*	*y*	*z*
Ir	1 501.9(8)	2 917.2(7)	2 237.5(3)	C(126)	752(20)	5 560(16)	1 251(9)
P(1)	2 763(5)	4 170(4)	1 502(2)	C(121)	2 001(18)	5 303(15)	1 101(8)
P(2)	2 196(5)	4 197(4)	3 186(2)	C(132)	4 304(18)	6 349(14)	2 082(8)
B(2)	1 185(24)	792(16)	2 186(11)	C(133)	5 514(26)	7 214(20)	2 251(11)
C(1)	538(19)	1 323(13)	2 780(9)	C(134)	6 754(25)	6 912(21)	2 140(10)
B(3)	−587(28)	2 196(17)	2 741(9)	C(135)	6 870(20)	5 772(20)	1 851(10)
B(7)	−936(25)	3 082(20)	1 975(10)	C(136)	5 650(19)	4 892(18)	1 684(11)
B(10)	41(24)	2 447(22)	1 312(11)	C(131)	4 380(17)	5 170(14)	1 769(8)
C(6)	835(19)	1 215(13)	1 443(8)	C(212)	207(21)	5 617(17)	3 169(9)
B(13)	−1 797(22)	1 875(20)	1 388(12)	C(213)	−292(25)	6 723(20)	3 198(9)
B(12)	−762(25)	878(20)	1 067(12)	C(214)	530(35)	7 829(23)	3 269(11)
B(9)	−406(25)	−96(19)	1 640(10)	C(215)	1 856(30)	7 842(22)	3 377(13)
B(5)	−1 119(24)	480(20)	2 476(12)	C(216)	2 470(22)	6 823(17)	3 347(11)
B(8)	−2 055(28)	1 717(23)	2 262(12)	C(211)	1 623(20)	5 672(17)	3 245(8)
B(11)	−1 965(26)	372(21)	1 683(10)	C(222)	4 373(26)	5 378(22)	4 033(10)
C(01)	6 259(30)	594(21)	3 851(12)	C(223)	5 730(26)	5 581(23)	4 259(10)
Cl(11)	4 773(10)	611(8)	3 396(5)	C(224)	6 712(27)	5 018(24)	3 962(11)
Cl(21)	6 407(14)	−901(13)	3 956(5)	C(225)	6 396(25)	4 204(22)	3 380(10)
Cl(31)	6 224(18)	1 561(16)	4 576(7)	C(226)	5 029(24)	4 016(20)	3 116(9)
C(112)	4 069(19)	2 310(15)	989(9)	C(221)	4 021(19)	4 600(16)	3 450(9)
C(113)	4 407(22)	1 535(19)	466(11)	C(232)	568(23)	3 801(20)	4 336(10)
C(114)	4 009(25)	1 550(23)	−170(10)	C(233)	165(28)	3 122(25)	4 891(12)
C(115)	3 168(24)	2 337(20)	−333(10)	C(234)	793(25)	2 181(22)	5 024(10)
C(116)	2 818(20)	3 164(19)	188(9)	C(235)	1 835(22)	1 829(19)	4 631(10)
C(111)	3 260(18)	3 138(15)	831(9)	C(236)	2 228(21)	2 491(18)	4 080(9)
C(122)	2 731(22)	5 972(18)	643(9)	C(231)	1 588(18)	3 464(16)	3 927(7)
C(123)	2 195(23)	6 810(20)	313(9)	O(13)	2 220(13)	88(11)	2 287(6)
C(124)	945(22)	7 056(17)	491(10)	C(43)	2 803(24)	−161(22)	1 776(12)
C(125)	223(22)	6 445(18)	952(11)				

Table 5. Final atomic co-ordinates (× 10^4) for compound (**3**)

Atom	*x*	*y*	*z*	Atom	*x*	*y*	*z*
Pt	2 366.7(5)	1 354.4(4)	981.3(6)	C(115)	3 877(21)	−1 057(21)	2 172(23)
P(1)	3 701(3)	757(2)	1 154(4)	C(116)	4 003(16)	−443(11)	2 204(18)
P(2)	3 135(4)	1 976(3)	−149(4)	C(121)	4 569(13)	948(13)	2 458(17)
C(2)	872(17)	710(12)	619(20)	C(122)	5 584(15)	853(15)	2 445(19)
C(3)	621(12)	1 363(11)	12(15)	C(123)	6 243(14)	1 007(12)	3 448(20)
B(4)	1 084(15)	1 954(10)	1 103(20)	C(124)	5 998(16)	1 306(16)	4 397(20)
B(5)	1 576(18)	1 573(13)	2 511(21)	C(125)	5 008(17)	1 446(17)	4 364(18)
B(6)	1 559(17)	750(14)	2 089(19)	C(126)	4 310(14)	1 281(14)	3 389(19)
B(7)	278(18)	543(11)	1 727(22)	C(211)	3 352(12)	2 771(12)	401(16)
B(8)	−332(16)	944(13)	443(22)	C(212)	3 678(14)	3 328(14)	−293(19)
B(9)	−163(16)	1 736(12)	744(20)	C(213)	3 892(18)	3 811(18)	172(23)
B(10)	354(20)	1 854(12)	2 261(24)	C(214)	3 824(21)	3 963(21)	1 356(26)
B(11)	650(18)	1 106(12)	2 869(20)	C(215)	3 501(19)	3 499(19)	2 038(23)
B(12)	−452(20)	1 218(14)	1 873(23)	C(216)	3 282(14)	2 906(10)	1 603(18)
C(10)	4 310(14)	931(10)	−101(17)	C(221)	2 542(12)	2 068(9)	−1 678(14)
C(20)	4 323(13)	1 654(10)	−201(16)	C(222)	3 014(14)	2 032(14)	−2 669(17)
C(111)	3 595(14)	−85(14)	1 174(17)	C(223)	2 517(16)	2 112(16)	−3 800(21)
C(112)	3 066(15)	−3 945(15)	183(19)	C(224)	1 527(18)	2 245(12)	−3 999(22)
C(113)	2 973(15)	−1 033(11)	147(20)	C(225)	1 103(17)	2 324(12)	−3 047(23)
C(114)	3 382(16)	−1 373(14)	1 141(23)	C(226)	1 565(15)	2 269(12)	−1 928(18)

was stirred for 0.5 h and then filtered. On exposure to air the filtrate showed a gradual colour change to a straw colour. Thin-layer chromatography (silica gel) using CH_2Cl_2 as eluant indicated the presence of the major yellow product [(dppe)-$PdC_2B_{10}H_{12}$] (**1**) at R_f 0.8, and a minor unidentified yellow component at R_f 0.6.

The complex [(dppe)$PdC_2B_{10}H_{12}$] was isolated by flash chromatography (silica gel) using CH_2Cl_2 as eluant, and was recrystallised from the same solvent (yield of yellow crystals 160 mg, 10%) (Found: C, 50.4; H, 5.65. Calc. for $C_{28}H_{36}B_{10}P_2Pd\cdot 0.5CH_2Cl_2$: C, 49.5; H, 5.40%). Since the calculated analysis for the crystalline material containing 1.0 CH_2Cl_2 gives C, 47.3; H, 5.2%, we assume that the crystals slowly lose solvent on standing.

Preparation of [$(PPh_3)_2HIrC_2B_{10}H_{11}(OMe)$] (**3**).—The compounds [NMe_4][$C_2B_{10}H_{13}$] (0.12 g, 0.65 mmol) and [$IrCl(PPh_3)_3$] (0.66 g, 0.65 mmol) were refluxed for 24 h in a mixture of degassed light petroleum (b.p. 60—80 °C, 45 cm^3) and methanol (25 cm^3). The colour of the mixture gradually changed from red to reddish brown, and a pale yellow solid was precipitated. After filtration the pale yellow solid was purified by preparative t.l.c. and was eluted with $CHCl_3$. After recovery from the plate the yellow solid was recrystallised from $CHCl_3$

(yield 80 mg, 16%) (Found: C, 47.6; H, 4.50. Calc. for $C_{39}H_{45}B_{10}IrOP_2 \cdot CHCl_3$: C, 47.5; H, 4.60%).

Preparation of Thallium(I) *Salt from* $[C_2B_{10}H_{12}]^{2-}$, *Formulated as* $Tl_3(C_2B_9H_{12})O$.—The carborane 1,2-$C_2B_{10}H_{12}$ (1.00 g, 6.9 mmol) was dissolved in thf (50 cm^3) containing small pieces of sodium (0.32 g, 13.8 mmol) and a trace of naphthalene. After stirring for 2—3 h to complete the reaction, thallium(I) acetate (3.63 g, 13.8 mmol) was dissolved in boiling ethanol (400 cm^3), and allowed to cool to 30—40 °C. The solution of $Na_2[C_2B_{10}H_{12}]$ was added to this stirred solution over 15 min, and the resulting fine orange precipitate was cooled to 0 °C and filtered. The product was washed with water (2 × 10 cm^3) and ethanol (2 × 10 cm^3), and finally with several portions of diethyl ether before being dried under vacuum. The product [0.87 g, 25% based on $Tl(O_2CMe)$] was then stored under vacuum at 0 °C (Found: C, 2.90; H, 1.45; B, 13.85; Tl, 83.9. Calc. for $C_2H_{12}B_9OTl_3$: C, 3.15; H, 1.60; B, 12.8; Tl, 80.4%).

Preparation of $[PMePh_3][C_2B_9H_{12}]$.—The orange $Tl_3(C_2B_9H_{12})O$ (0.50 g, 0.66 mmol) and $[PMePh_3]Br$ (0.24 g, 0.66 mmol) were mixed in thf (40 cm^3) and stirred for 1 h. The resulting black suspension was removed by filtration, and the air-stable pale yellow filtrate was evaporated under vacuum to yield an oil residue. The residue was dissolved in $CHCl_3$ (10 cm^3), and the pale yellow product was precipitated by the addition of excess of light petroleum (b.p. 60—80 °C). After filtration, and washing with light petroleum, the solid was dried under vacuum (yield 0.19 g, 70%) (Found: C, 59.6; H, 7.50. Calc. for $C_{21}H_{30}B_9P$: C, 61.4; H, 7.35%). The ^{11}B n.m.r. spectrum was recorded from an acetone solution.

Preparation of $[(dppe)PtC_2B_9H_{11}]$ (**3**).—A suspension of the orange solid $Tl_3(C_2B_9H_{12})O$ (0.50 g, 0.66 mmol) was stirred and refluxed in thf (20 cm^3) for 0.5 h. The resulting pale orange precipitate was removed from the deep red supernatant by filtration. The solution was evaporated to an oil which was dissolved in $CHCl_3$ (10 cm^3). Cooling to −78 °C followed by the addition of excess of diethyl ether yielded a light brown solid which was collected after filtration. Thin-layer chromatography showed this material to be a mixture of products, but the compound $[(dppe)PtC_2B_9H_{11}]$ was isolated as one of the major components by flash chromatography using $CHCl_3$–light petroleum (b.p. 60—80 °C) (75:25 by volume) as eluant. Crystals suitable for *X*-ray crystallography were obtained by recrystallisation from acetone–CH_2Cl_2 (yield of crystals 30 mg, 6.3%).

Crystal-structure Analyses.—Crystal data and collection and refinement parameters are given in Table 2. Data were collected with a Syntex $P2_1$ four-circle diffractometer in θ—2θ mode with scan speed from the specified minimum to 29° min^{-1}, depending on the intensity of a 2-s pre-scan; backgrounds were measured at each end of the scan for 0.25 of the scan time. For (**2**), reflections with $2\theta > 35°$ were only collected if they exceeded a set count on an 8-s pre-scan. For (**3**), the crystal was held at −100 °C with the Syntex LT-1 attachment. Three standard reflections were monitored every 200 reflections, and any slight changes during data collection were corrected by rescaling. Density was measured by flotation. Unit-cell dimensions and standard deviations were obtained by least-squares fit to 15 high-angle reflections. Only observed reflections $[I/\sigma(I) \geq 3.0]$ were used in refinement, corrected for Lorentz, polarisation and absorption effects, the last with ABSCOR.[15]

For each compound, the heavy atom was located by Patterson techniques and the light atoms were then found on successive Fourier syntheses. Hydrogen atoms were given fixed isotropic thermal parameters, inserted at calculated positions and not refined; the hydrogens of the methyl group of (**2**) were omitted as was its hydride ligand. Compound (**1**) was found to contain a highly disordered CH_2Cl_2 molecule, which was approximated by two Cl atoms with occupancy 0.7, and five carbon atoms with fixed co-ordinates and thermal parameters (0.10 $Å^2$), and occupancies refined to 0.5—0.1; it still had residual peaks up to 2 e $Å^{-3}$ in the neighbourhood of the solvent. Compound (**2**) contained a molecule of $CHCl_3$, given occupancy 0.7. Final refinement was by cascaded least-squares methods, with anisotropic thermal parameters for all atoms other than hydrogen and some solvent atoms.

The positions of the cage carbon atoms were identified principally by their shorter bonds, though the behaviour of their thermal parameters on refinement was used in confirmation. A weighting scheme of the form $w = 1/[\sigma^2(F) + gF^2]$ was used for (**1**) and (**2**); (**3**) was given unit weights, and all weighting schemes were checked by weight analysis. Computing for (**1**) and (**2**) was with the SHELXTL system[16] on a Data General NOVA3, following initial processing on a Burroughs B6800 computer; for (**3**), *X*-RAY 76 was used.[17] Scattering factors in the analytical form and anomalous dispersion factors were taken from ref. 18. Final atomic co-ordinates are given in Tables 3—5. For (**3**), F_o/F_c tables could not be produced because of a loss of data files, but absorption-corrected F_o data are available on request to the authors.

Acknowledgements

We thank the S.E.R.C. for support of this work.

References

1 N. N. Greenwood, *Chem. Soc. Rev.*, 1984, **13**, 353; R. N. Grimes, in 'Comprehensive Organometallic Chemistry,' eds. G. W. Wilkinson, F. G. A. Stone, and E. W. Abel, Pergamon, Oxford, 1982, vol. 1, p. 459; J. D. Kennedy, *Prog. Inorg. Chem.*, 1984, **32**, 519.
2 H. M. Colquhoun, T. J. Greenhough, and M. G. H. Wallbridge, *J. Chem. Soc., Dalton Trans.*, 1985, 761 and refs. therein.
3 G. B. Dunks, R. J. Wiersema, and M. F. Hawthorne, *J. Am. Chem. Soc.*, 1973, **95**, 3174 and refs. therein.
4 D. F. Dustin, G. B. Dunks, and M. F. Hawthorne, *J. Am. Chem. Soc.*, 1973, **95**, 1109.
5 C. G. Salentine and M. F. Hawthorne, *Inorg. Chem.*, 1976, **15**, 2872.
6 F. Y. Lu, C. E. Strouse, K. P. Callahan, C. B. Knobler, and M. F. Hawthorne, *J. Am. Chem. Soc.*, 1975, **97**, 428.
7 M. R. Churchill and B. G. DeBoer, *Inorg. Chem.*, 1974, **13**, 1411.
8 J. L. Spencer, M. Green, and F. G. A. Stone, *J. Chem. Soc., Chem. Commun.*, 1972, 1178.
9 H. Fowkes, N. N. Greenwood, J. D. Kennedy, and M. Thornton-Pett, *J. Chem. Soc., Dalton Trans.*, 1986, 517.
10 D. V. Howe, C. J. Jones, R. J. Wiersema, and M. F. Hawthorne, *Inorg. Chem.*, 1971, **10**, 2516.
11 W. R. Miller, L. G. Sneddon, D. C. Beer, and R. N. Grimes, *J. Am. Chem. Soc.*, 1974, **96**, 3090.
12 D. M. P. Mingos, M. I. Forsyth, and A. J. Welch, *J. Chem. Soc., Dalton Trans.*, 1978, 1363.
13 M. J. Hudson, R. S. Nyholm, and M. H. B. Stiddard, *J. Chem. Soc. A*, 1968, 40.
14 M. A. Bennett and D. L. Milner, *J. Am. Chem. Soc.*, 1969, **91**, 6983.
15 N. W. Alcock, in 'Crystallographic Computing,' ed. F. Ahmed, Munksgaard, Copenhagen, 1970.
16 G. M. Sheldrick, SHELXTL User Manual, Nicolet Instrument Co., Madison, Wisconsin, 1981.
17 J. M. Stewart, Technical Report TR-446, Computer Science Centre, University of Maryland, 1976.
18 'International Tables for *X*-Ray Crystallography,' Kynoch Press, Birmingham, 1974, vol. 4.

Received 5th June 1986; *Paper* 6/1127